

Improvement on the Acoustic Performance of Internal Combustion Forklift Intake System by the Finite Element Method

ZHIGANG WANG^{1,a}, ZEYU WENG^{1,b}, SUYI SHEN^{1,2,c}, MINGHUI LI², XIAOQING SHEN²
SHUFENG XIANG²

¹College of Mechanical Engineering, Zhejiang University of Technology, Hangzhou 310014,
CHINA

²Hangcha Group Co.Ltd, Hangzhou 311305, CHINA

^awangzg213@126.com, ^bwengzy8888@163.com, ^cssywork@163.com

Abstract: - This paper took the intake system of an internal combustion forklift as a whole, defined the filter core in air filter as a porous media characterized by geometrical and property parameters, and simulated perforated plate by creating acoustic impedance relationship between front and rear of perforated plate. According to the air intake noise test results of the internal combustion forklift, the improved scheme of intake system was proposed. The finite element models of intake system were established by the finite element method, and then their transmission losses were obtained. The comparison of the transmission losses showed that the acoustical performance of intake system was improved efficiently. Finally, the internal combustion forklift vehicle noise test was carried out; the test results showed that noise sound pressure level at ears were obviously reduced by improved intake system. Thus, this method is feasible and can be used for improvement on the acoustic performance of intake system.

Keywords: - Internal combustion forklift, intake system, acoustic performance, finite element method, improvement

1 Introduction

Internal combustion forklift (IC forklift) is an engineering vehicle which is used for transporting materials. It is an important equipment to realize the modernization of logistics, lighten the handling strength of workers and improve the efficiency. However, its noise not only has a bad influence on driver and surrounding operators, but also seriously hinders the further development [1]. The overall noise level of IC forklift is made up of contributions from many noise sources such as engine intake system, exhaust system, cooling fan, hydraulic

system, and engine radiation. Usually the intake system is responsible for 25–50% of the overall noise [2]. Intake system is a major noise source of the IC forklift. Therefore it is an effective method to reduce IC forklift noise by improving the silencer performance of intake system.

In this paper, IC forklift intake system composes of column, flexible tube, air intake muffler, air filter, connection tube and etc, as in Fig.1. The acoustic attenuation performance of overall intake system is affected by each component performance. Many scholars have conducted some researches on the acoustic attenuation performance of air intake

muffler, air filter and connection tube. However, most of the research is only restricted to the acoustic attenuation performance of a component itself. As the acoustic performance of intake system components are interrelated and influenced each other, the paper will take the intake system as a whole to improve.



Fig. 1 the components of IC forklift intake system

Since the IC forklift intake system has complex internal structure and the plane wave regime is only established at low frequencies. So, the plane wave theory is not applicable to analyze the intake system noise. There will be the relatively large error using traditional methods to calculate. However, finite element method can accurately predict the acoustic attenuation performance of complicated system at higher frequencies. A correct and reasonable acoustic finite element model determines the reliability of simulation. There are mainly two difficulties to create the acoustic finite element model of IC forklift intake system. The first difficulty is the establishment of the filter core material model in air filter. If simulation ignores the impedance characteristics of the filter core material, the results will appear the large error. Furthermore, the dissipative materials cannot be regarded as a rigid body structure model directly; it is need to put filter core domain independent and divide continuous mesh, and set the property parameters of equivalent relationship between the filter core material and air. The second difficulty is the establishment of finite element model of perforated plate. The size and layout of perforations effectively influence the

simulation accuracy and efficiency. For the perforated plate with many small size holes, the perforated plate model established directly will increase the grid and node number and affect the computational efficiency. Therefore, this paper needs to establish acoustic impedance relationship between front and rear of the perforated plate to simulate perforated structure.

For the above two problems, many scholars have conducted some researches. For example, JIA [3] experimentally obtained the filter core material parameters of air filter, used the obtained parameters to equivalently substitute filter core, and verified the feasibility of the equivalent method in finite element software. Jin [4] improved the structure of air filter and took advantage of computer simulation software to calculate the TL, and experimentally proved the correctness of the filter core material setting method. Sullivan and Crocker [5] measured the impedance of perforated elements in a concentric tube resonator and then gave the empirical formula of perforations acoustic impedance. Later, Lee and Selamet [6] improved the experiment of Sullivan, measured impedance of perforated plates having four different perforation rates, proposed the terminal correction coefficient of empirical formula of perforated plate acoustic impedance. Sun et al [7] created a perforated plate model and analyzed its acoustic performance by using the finite element method. The computation results are compared with that of the traditional model. It is found that the finite element method can be a good candidate to solve perforation problem.

Based on the modeling method of air filter and perforated plate, this paper creates the finite element model of the overall intake system. According to the test results, this paper put forward to the improvement scheme of the overall intake system, and verifies the feasibility of the improved scheme through the IC forklift vehicle noise test.

2 The Acoustic Attenuation Perform-

Performance and Finite Element Model

Establishment of Air Filter

2.1 The acoustic attenuation performance of air filter

Air filter acoustically belongs to an expansion chamber muffler and contains filter core material that not only has the function of cleaning air but also a certain sound-absorbing effect. Therefore, air filter can be regarded as a hybrid silencer designed by combining dissipative and reflective components.

Dissipative muffler usually makes use of porous absorbing material with different structures to absorb sound energy and reduce the noise level. It has good acoustic attenuation effect of high frequency noise [8]. The sound absorption performance of the porous material is affected by many factors such as material geometrical and property parameters; the material structure parameters include flow resistance, porosity and geometrical factor; in addition, the material property parameters include material density and the speed of sound wave propagation in the material.

Filter paper in air filter belongs to a fibrous material of porous sound-absorbing material; it can effectively absorb high frequency noise. Based on the acoustic theory of absorption material, porous material can be equivalently replaced by fluid when the skeleton of porous medium is in the stationary state. The expressions on the plural wave number ratio and impedance ratio of sound-absorbing material are [9]:

When $E \leq 0.025$,

$$k / k_0 = (1 + 0.136E^{-0.641}) - j0.322E^{-0.502} \quad (1)$$

$$Z / Z_0 = (1 + 0.081E^{-0.699}) - j0.191E^{-0.556} \quad (2)$$

When $E > 0.025$,

$$k / k_0 = (1 + 0.103E^{-0.716}) - j0.179E^{-0.663} \quad (3)$$

$$Z / Z_0 = (1 + 0.0563E^{-0.699}) - j0.127E^{-0.655} \quad (4)$$

Where k and Z are the equivalent wave number and impedance, respectively; k_0 and Z_0 are the air wave

number and impedance, respectively; $E = q_0 f / R$, is a nondimensional parameter; q_0 is air density; f is frequency; R is material flow resistivity, $Rayls/m$.

2.2 The finite element model establishment of air filter

As for the finite element model of air filter, it is significant to establish the geometrical model of filter core material. The paper determines the geometrical and property parameters for the porous material by solving the equivalent simulation relationship between porous materials and air.

In order to define filter core material geometrical and property parameters, meantime, keep the continuity of elements, this paper set the filter core domain on the established finite element model of intake system inner field; the specific means is that the intake system inner field model is imported into Hypermesh software and is divided to make the filter core domain independent from the entire model, then, the filter core domain is set to different mesh property with the rest of the intake system inner field model. This method can keep complete boundary between properties, and will not affect the continuity of the elements. The article import the mesh generated into acoustic calculating software, and input the parameters (such as sound velocity, air density, geometrical factor, and porosity, flow resistivity) in the absorbent material property of filter core domain directly before calculation. The filter core material parameters are shown in table 1.

Table 1 the filter element material parameters

Parameters	Value
Sound velocity(m/s)	340
Air density(kg/m^3)	1.225
Geometrical factor	2
Porosity	0.95
Flow resistivity($Rayls/m$)	5000

3 The Acoustic Attenuation Performance and Finite Element Model

Establishment of Perforated Plate

3.1 The acoustic attenuation performance of perforated plate

Perforated plate structure takes use of perforations and cavity to play the silencing effect. It is a kind of low quality and high impedance resonance silencing structure. The structure of perforated plate is shown in Fig. 2.

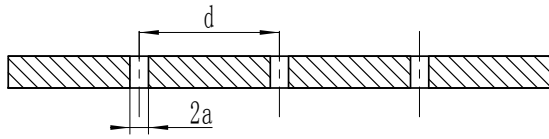


Fig. 2 the structure of perforated plate

The linear relationship between the acoustic pressure and volume velocity front and rear of the perforated plate is given by Eq. (5).

$$\begin{bmatrix} v_{n1} \\ v_{n2} \end{bmatrix} = \begin{bmatrix} \alpha_1 & \alpha_2 \\ \alpha_4 & \alpha_5 \end{bmatrix} \begin{bmatrix} p_1 \\ p_2 \end{bmatrix} + \begin{bmatrix} \alpha_3 \\ \alpha_6 \end{bmatrix} \quad (5)$$

Where v_{n1} and v_{n2} are the normal vibration velocity in front and rear of the perforated elements, respectively; p_1 and p_2 are sound pressure in front and rear of the perforated elements, respectively; $\alpha_1, \alpha_2, \alpha_4$ and α_5 are transmission admittance coefficient; α_3 and α_6 that are related to sound source are equal to zero [10].

When sound pass the perforated plate, perforations have certain inhibition effect to sound; this effect is called acoustic impedance calculated by Eq. (6).

$$Z_p = \frac{\Delta p}{V} = R_p + j \cdot X_p \quad (6)$$

Where Δp is the pressure difference between front and rear of the perforated elements; V is the averaged particle velocity in the holes.

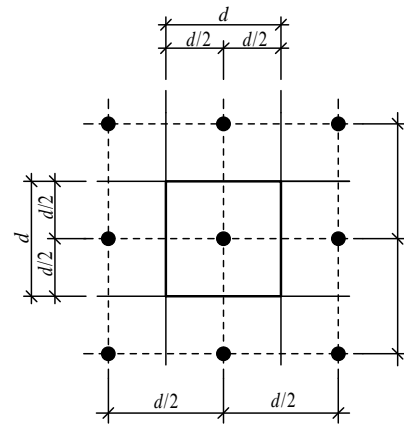
When the thickness l of perforated plate satisfies equation of $l \ll 4a$, the real part R_p and imaginary part X_p of impedance can be represented as:

$$R_p = \frac{1}{\varepsilon} \sqrt{8 \cdot \omega \cdot \eta \cdot \rho} \left(1 + \frac{l}{2a} \right) \quad (7)$$

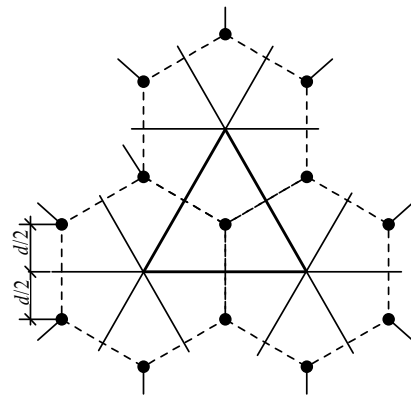
$$X_p = \frac{1}{\varepsilon} \cdot \omega \cdot \rho \cdot (l + 2\Delta l) \quad (8)$$

Where ε is the perforation rate of perforated plate; $\omega = 2\pi f$, is angular frequency; a is the radius of hole; η is the dynamic viscosity of fluid; ρ is the density of fluid; Δl is correction coefficient.

There are two kinds of arrangements of perforations center in engineering, as in Fig. 3.



(a) Square



(b) Regular hexagon

Fig. 3 the arrangement of holes center

For the case of the Fig. 3(a)

$$\varepsilon = \frac{\pi \cdot a^2}{d^2} \quad (9)$$

$$\Delta l = \begin{cases} 0.85 \cdot a \cdot \left(1 - 2.34 \frac{a}{d} \right), & 0 < \frac{a}{d} \leq 0.25 \\ 0.668 \cdot a \cdot \left(1 - 1.9 \frac{a}{d} \right), & 0.25 < \frac{a}{d} < 0.5 \end{cases} \quad (10)$$

For the case of the Fig. 3(b)

$$\varepsilon = \frac{6\pi \cdot a^2}{5\sqrt{3}d^2} \quad (11)$$

$$\Delta l = \begin{cases} 0.85 \cdot a \cdot \left(1 - 2.52 \frac{a}{d}\right), & 0 < \frac{a}{d} \leq 0.25 \\ 0.668 \cdot a \cdot \left(1 - 2.0 \frac{a}{d}\right), & 0.25 < \frac{a}{d} < 0.5 \end{cases} \quad (12)$$

Where d is the distance between the centers of adjacent perforations.

3.2 The finite element model establishment of perforated plate

As for the finite element model of perforated plate, it is usual to simulate perforation structure by setting a continuous uniform impedance boundary. As the diameter of every hole is small in the perforated plate, it cost much time to mesh and compute. Therefore, the simulation can be replaced by transmission admittance matrices instead of setting up the grid model of perforated plate. The transmission admittance matrix is given by Eq. (13).

$$\begin{bmatrix} \beta & -\beta \\ -K\beta & K\beta \end{bmatrix} \quad (13)$$

Where K is the impact factor of perforated plate thickness on the area on both sides of perforated plate; β is perforated admittance, $\beta = \frac{1}{Z_p}$.

In the process of acoustic calculation, as the transmission admittance values are different with frequencies, this paper calculate the real and imaginary part of impedance corresponding frequency according to Eq. (7) and Eq. (8) and list a table. In the paper, the arrangement of holes center is regarded as the regular hexagon. The perforated plate parameters are plotted in table 2. This paper set mesh groupings in front and rear of the perforated plate mesh model, and defines admittance relations between the mesh groupings by editing the transmission admittance matrix. At last, the finite element model of the perforated plate structure is established.

Table 2 the perforated plate parameters

Parameters	Value
Perforated plate thickness (m)	0.001
Hole diameter (m)	0.001
Adjacent holes center distance (m)	0.005
Perforation rate	0.031416
Correction coefficient	2.67×10^{-4}
Fluid density (kg/m^3)	1.225
Fluid dynamic viscosity (Pa/s)	1.71×10^{-5}

4 Acoustic Finite Element Simulation

4.1 Finite element model establishment

Fig. 4 shows the established inner field model of the intake system by using the CATIA V5 software. The acoustic wave caused by the alternate openings and closings of the cylinder intake valves propagate along the intake system at the speed of sound, and radiate noise to the environment through the inlet section of the intake system [10].

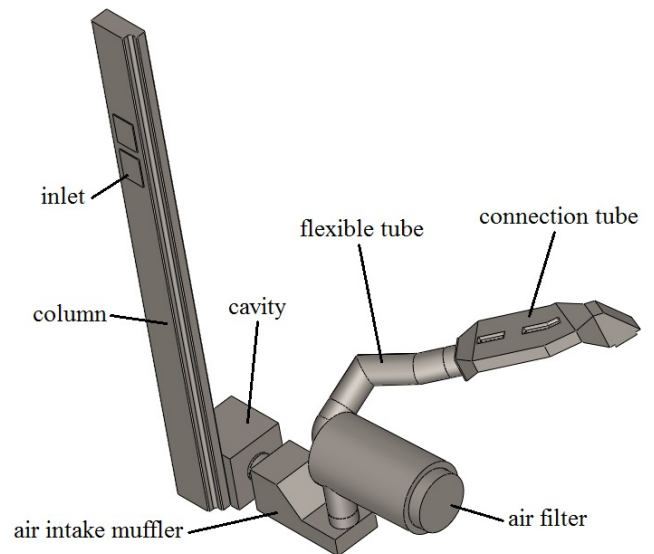


Fig. 4 the inner field model of intake system

The inner field model of the intake system is imported into Hypermesh software to create the finite element model. When the mesh of the finite element model of the intake system is divided into dense mesh, a large number of nodes and elements for the intake system will greatly reduce the computational efficiency of software; when the mesh

of the finite element model of the intake system is divided into coarse mesh, the relatively large error of computation is to be produced. Generally, for the linear finite element model, the edge length of the largest element should be 1/6 less than the shortest wavelength of the calculated frequency. The maximum edge length of the mesh cell of the finite element model can be obtained by Eq. (14) [11]:

$$L_{\max} \leq \frac{1}{6} \frac{c}{f_{\max}} \quad (14)$$

Where c is sound velocity; f_{\max} is the maximum calculated frequency.

From the Eq. (14), we can see when the frequency increases, the edge length of element will become small, and the number of elements and computation time will increase; so the maximum frequency should be reasonably determined. Due to the intake noise frequency of diesel engine mainly concentrates within 1000 Hz, thus the maximum size of element should not exceed 56.7 mm. In addition, because of the complexity of the intake system internal structure, the large element size will easily cause mesh distortion. After comprehensively considering the above factors, this paper set element size of 7 mm.

4.2 Boundary condition

Generally speaking, muffler is contained in intake system and exhaust system of an IC forklift. The performance of a muffler is measured in terms of the transmission loss (TL), insertion loss (IL).

Transmission loss requires an anechoic termination at the downstream end; it is defined as the difference between the sound power level incident on the muffler and that transmitted downstream into an anechoic termination; it just shows the transfer characteristics of the muffler structure itself, which has nothing to do with external factors such as sound source. The transmission loss of the intake system can be approximately regarded as the superposition that of each silencing components, but is not a simple linear superposition [12]. Therefore, transmission loss is regarded as evaluation of simulation results. Symbolically,

$$TL = L_{W_{in}} - L_{W_{out}} = 10 \lg \left(\frac{W_{in}}{W_{out}} \right) \quad (15)$$

$$= 10 \lg \left[\frac{(p_{in} + v_n \rho c)^2 A_{in}}{4 p_3^2 A_{out}} \right]$$

Where $L_{W_{in}}$ is the incident sound power level; $L_{W_{out}}$ is the sound power level into an anechoic termination; W_{in} is the incident sound power; W_{out} is the sound power into an anechoic termination; p_{in} is the incident sound pressure; p_3 is the sound pressure into an anechoic termination; A_{in} and A_{out} are the inlet and outlet cross-sectional area; c is sound velocity; ρ is the medium density.

The paper applies acoustic calculating software to obtain the transmission loss of intake system. In this case, the simulation ignores the impact of wall on internal sound field, and the coupling action between fluid and rigid body. The boundary conditions are:

- (1) The wall is non-reflective rigid;
- (2) To impose a particle velocity of unit magnitude at the surface of inlet section; that is, $v_n = -1$, the minus describes the voice entry;
- (3) To set absorbent panel property at the surface of outlet section; that is, $\rho c = 416.5$.

4.3 Simulation result

In the paper, the calculation frequency is from 1Hz to 1000Hz, stepping for 3Hz. The obtained transmission loss of intake system is shown in Fig. 5.

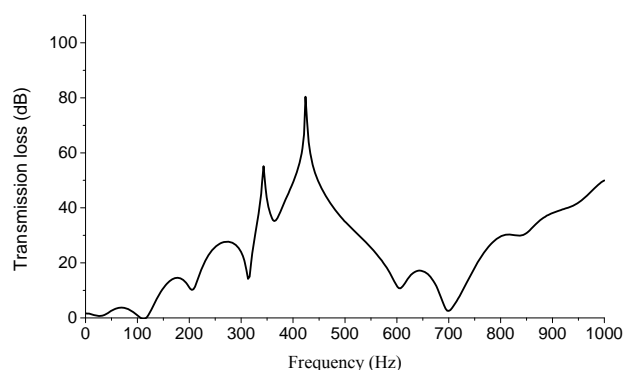


Fig. 5 the transmission loss of intake system

From the Fig. 5, it is noted that the acoustic attenuation effect is bad in the medium and high frequency band; especially, the sound reduction is

not ideal in the frequency band of 26 ~ 323 Hz and 323 ~ 778 Hz, and there are many passing frequencies. Thus it is need improvement on two frequency bands in order to improve the amount of noise elimination.

5 Intake System Improvement

The induction noise of intake system is measured by LMS test.lab test system. According to the test data, we conclude that the frequency bands greatly contributing to induction noise are 60~100Hz, 250~350Hz and 500~800Hz. The key frequencies are 87Hz, 320Hz, 596Hz, 659Hz, 750Hz and 890Hz. Based on the test results, this paper improve the structure of air intake muffler, air filter and connection tube, respectively. The specific improved design schemes are:

- (1) to enlarge the volume of air intake muffler, and obtain the biggest expansion ratio as far as possible; to install insertion tube at the inlet in order to eliminate partial passing frequency;
- (2) to increase the cavity length to obtain better low-frequency acoustical attenuation effect;
- (3) to design the perforated plate resonance structure in view of the key frequencies.

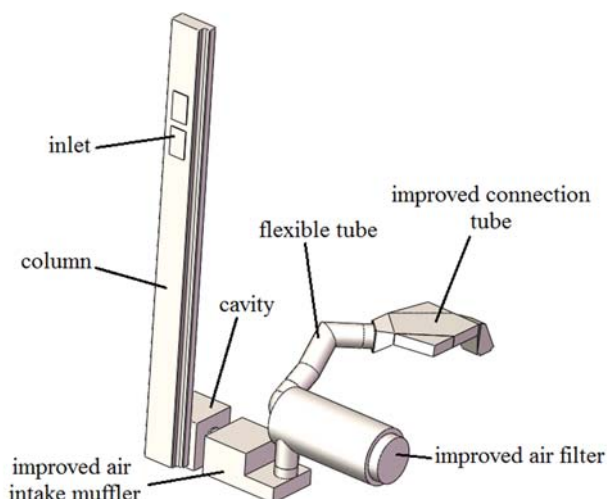


Fig. 6 the inner field model of improved intake system

Simulation analysis of the improved intake

system was carried out. The comparison of TL of the original and improved intake system is shown in Fig. 7.

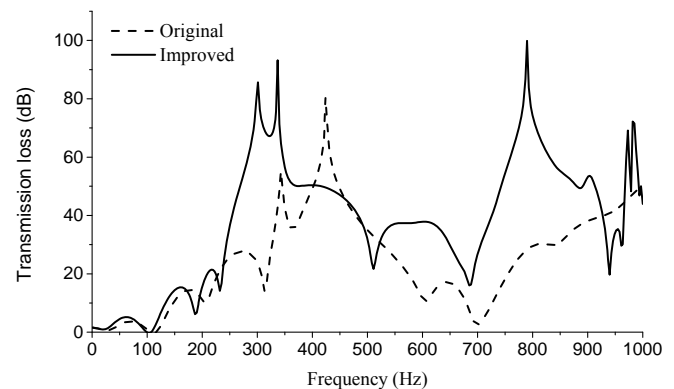


Fig. 7 the TL of the original and improved intake system

From the Fig. 7, it can be found that the TL curve of the improved intake system is higher than the original intake system. The muffling ability over the frequency range of 280~340Hz and 750~850Hz of the improved structure is obviously stronger than the original structure. Even the sound reductions are lower than the original intake system in some frequencies, but the sound reductions at overall frequency bands has been greatly improved. So the simulation results can meet requirement of design.

6 Experimental Study of the Improved Intake System

According to the standard of counterbalanced fork-lift trucks-testing method for whole machines [13], this paper proposes an experimental scheme about the noise test of the IC forklift vehicle in order to study the acoustic attenuation effect of the improved intake system. The measuring instrument is the LMS test.lab device of Siemens Company. This device is composed of microphone, data analysis software, PC and etc. The microphones are placed in the position where the height from the seat is $0.91\text{m} \pm 0.05\text{m}$ and the distance deviating from the driver center is $0.20\text{m} + 0.02\text{m}$. The measured

quantities are the sound pressure levels at ears in run-up, idle speed and operation conditions, respectively (see Table 3, Table 4).

Table 3 the A-level sound pressure at ears of forklift with original intake system

Ears	Run-up condition sound pressure level (dB)	Idle speed condition sound pressure level (dB)	Operation condition sound pressure level (dB)
Left ear	89.75	66.64	89.82
Right ear	89.09	66.23	90.25

Table 4 the A-level sound pressure at ears of forklift with improved intake system

Ears	Run-up condition sound pressure level (dB)	Idle condition sound pressure level (dB)	Operation condition sound pressure level (dB)
Left ear	87.27	65.46	86.63
Right ear	86.94	65.33	87.09

According to the test standard, this paper take overall consideration of the noise test values under the above three conditions. A-level radiation sound pressure is measured to determine the internal combustion forklift noise performance; computation formula is as follows:

$$L_{p_{AZ}} = 10 \lg \left[\frac{1}{a+b+c} \times \left(a \times 10^{0.1L_a} + b \times 10^{0.1L_b} + c \times 10^{0.1L_c} \right) \right] \quad (16)$$

Where a, b, c is the operating time factors in run-up, idle speed and operation conditions, respectively; their values are listed in table 5. L_{p_a} is the A-level sound pressure in run-up condition; L_{p_b} is the A-level sound pressure in idle condition; L_{p_c} is the A-level sound pressure in operation condition.

Table 5 the operating time factors

a	b	c
0.18	0.58	0.24

The A-level radiation sound pressure ($L_{p_{AZ}}$) at ears of forklift with original and improved intake system is shown in the Fig. 8.

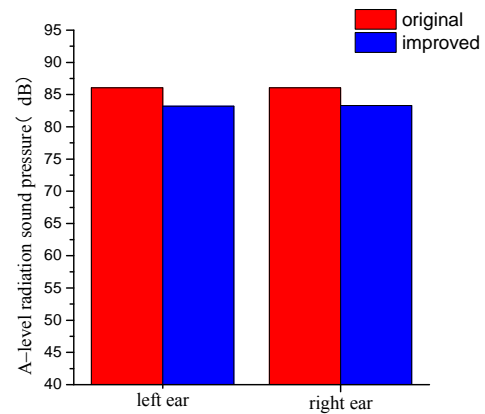


Fig. 8 the $L_{p_{AZ}}$ at ears of forklift with original and improved intake system

From the Fig. 8, we can find that the improved intake system has good silencing performance. The noise level of left ear reduces from 86.05dB to 83.19 dB and the noise level of right ear reduces from 86.05dB to 83.29dB. The improved intake system has good silencing effect on vehicle noise. It proves the validity of the intake system improvement and the effectiveness of the finite element method.

7 Conclusions

In this paper, the finite element method is used to calculate the transmission loss of IC forklift intake system; and the noise level at ears of the IC forklift vehicle is measured. The conclusions are:

- (1) The intake system as a whole is the premise to improve the acoustic performance of internal combustion forklift intake system.
- (2) The establishment of the finite element models of air filter and perforated plate is the key to the acoustic finite element simulation analysis of the internal combustion forklift intake system.

The comparison between simulation and test results verifies the correctness of the modeling method of air filter and perforated plate.

- (3) Finite element method can be used to evaluate the silencing performance of IC forklift intake system.
- (4) The improved intake system makes the noise level at ears of IC forklift reduce by 2.86dB and 2.76 dB, respectively.

References:

- [1] Yang Mingliang, Xu Gening, Vibration study of fork-lift truck based on the constraint rigid flexible coupling system. *Journal of mechanical engineering*, Vol.47, 2011, pp. 89-94.
- [2] Daniela Siano, Michela Costa and Fabio Bozza, Prediction and enhancement of the acoustic performance of a spark ignition engine intake air filter box. *Journal of automobile engineering*, Vol.227, No.4, 2013, pp. 591-604.
- [3] Jia Weixin, Research on numerical simulation of structural noise/intake noise and optimization design. Hangzhou: Zhejiang University, 2008.
- [4] Jin Xiaoxiong, Wu Yingjiang and Jin Chang. Improvement and experiment study of air filter noise control. *Machine Design and Research*, Vol.25, 2009, pp. 100-103.
- [5] Sullivan J W, Crocker M J. Analysis of concentric tube resonators having unpartitioned cavities. *The Journal of the Acoustical Society of America*, Vol.64, No.1, 1978, pp. 207-215.
- [6] Lee I, Selam et A. Acoustic impedance of perforations in contact with fibrous material. *Journal of the Acoustical Society of America*, Vol.119, No.5, 2006, pp. 2785-2797.
- [7] Sun Xinbo, Tang Honggang and Liu Lin et al. Acoustic Performance Analysis of Concentric-Tube Resonator with Perforated Baffle. *Noise and Vibration Control*, Vol.6, No.12, 2010, pp. 189-191.
- [8] Ma Dayou, Noise and vibration control engineering handbook, Science Press, Beijing, 2002.
- [9] Zhan Fuliang, Xu Junwei. Virtual lab acoustics simulation from entry to the master, Northwestern Polytechnical University Press, Xian, 2013.
- [10] Ji Zhenlin, *Acoustic Theory and Design of Muffler*. Beijing: Science Press. 2015, 291-292.
- [11] Xiaodong Li, Xintan Ma, *Mathematic Analysis and Performance Simulation for Exhaust Muffler Based on Transmission Loss*. *Applied Mechanics and Materials*. Vols. 651-653 (2014): 972-975.
- [12] Zheng Lei, *Structure Improvement and Acoustic Characteristics Analysis of Automobile Exhaust Muffler*. Chongqing: Chongqing University, 2009.
- [13] JB/T 3300-2010, "Counterbalanced fork-lift trucks-Testing method for whole machines" (Ministry of Industry and Information Technology of the People's Republic of China, Beijing, 2010).